Design of Three-Spatial-Mode Ring-Core Fiber

Motoki Kasahara, Kunimasa Saitoh, *Member, OSA*, Taiji Sakamoto, Nobutomo Hanzawa, Takashi Matsui, Kyozo Tsujikawa, and Fumihiko Yamamoto

***Abstract*—We investigate the fiber parameters which meet the design conditions for effectively three-spatial-mode transmission and low bending loss in a ring-core fiber for mode-division multiplexing transmission. We also clarify the effective area and the difference of the effective index while satisfying the design conditions.**

***Index Terms*—Differential mode delay, difference of the effective index, effective area, few-mode fiber, finite element method, mode-division multiplexing, ring-core fiber.**

I. Introduction

In order to satisfy the requirements of large transmission capacity, mode-division multiplexing transmission has been attracted as new generation optical fiber communication systems. Many mode-division multiplexing transmission systems using few-mode fibers have been proposed [1]–[4]. In regards to the number of propagation modes, Refs. [1], [2] support two linearly polarized (LP) modes (LP_{01}, LP_{11}), Ref. [3] supports three LP modes ($LP_{01}, LP_{11}, LP_{21}$), and Ref. [4] supports four LP modes ($LP_{01}, LP_{11}, LP_{21}, LP_{02}$). Additionally, Refs. [2]–[4] support degeneration modes and polarization modes. Crosstalk by mode coupling becomes large as the number of propagation modes increases. The crosstalk between propagation modes can be compensated by multiple input multiple output (MIMO) processing, but the computational complexity and power consumption of MIMO processing increase with increasing differential mode delay (DMD). Therefore, using the graded-index few-mode fibers with low DMD is the preferred approach [5], [6]. However, detailed design and precise fabrication process are required to realize desired characteristics. In contrast, by increasing the difference of the effective index ($\Delta n_{\rm eff}$) between propagation modes, it is possible to suppress mode coupling [7]. In more detail, the mode coupling is associated with micro-scale fluctuations in fiber diameter typically arising during the fiber drawing process or in response to random radial pressures. Therefore, the mode coupling greatly depends on manufacturing accuracy of the fiber and environmental conditions for cabling. However, if we compare several fibers having similar uniformity along the fiber length, the fiber with large $\Delta n_{\rm eff}$ is superior in reduction of mode coupling. Hence, using the uncoupled few-mode fibers with large $\Delta n_{\rm eff}$ is the second preferred approach [8].

Enlarging effective area ($A_{\rm eff}$) is also beneficial in reducing the nonlinear effects which degrade transmission characteristics. Several fibers with large $A_{\rm eff}$ have also been proposed [9], [10]. However, fibers with large $A_{\rm eff}$ are known to be micro-bending sensitive. For instance, micro-bending loss of the step-index fiber (SIF) with $A_{\rm eff}$ of 160 μm^2 is larger than 100 dB/km [11]. In this paper, we investigate the structural parameter dependence of $A_{\rm eff}$ in a ring-core fiber (RCF) supporting three spatial modes in order to control the $A_{\rm eff}$ to a desired value.

Recently, RCFs for mode-division multiplexing transmission have been proposed. Ref. [12] supports two LP modes (LP_{01}, LP_{11}) and Ref. [13] supports four LP modes ($LP_{01}, LP_{11}, LP_{02}$, LP_{22}). Here, the LP_{02} and LP_{22} modes only exist in RCF if the ring width is large enough to radially support multimode. The number of radial modes and the number of azimuthal modes are slightly independent. The azimuthal number of propagation modes depends on radius and thickness of the ring layer, while the radial number of propagation modes depends on only thickness of the ring layer [14]. In this paper, we consider RCFs with three spatial modes (LP_{01}, LP_{11}, LP_{21}). If we consider degeneration modes and polarization modes, the three-spatial-mode fiber supports ten modes (LP_{01}: two modes, LP_{11}: four modes, LP_{21}: four modes). Besides, we do not want to use LP_{02} mode. Both LP_{01} and LP_{02} modes have a field distribution having a peak in the center of the core. Therefore, in addition to mode coupling in a transmission fiber, large mode conversion between LP_{01} and LP_{02} modes will occur at a discontinuous point.

In this paper, we investigate the fiber parameters that support three-spatial-mode under constraints on the bending loss (BL) of propagation modes, and the structural parameter dependence of $\Delta n_{\rm eff}$ and $A_{\rm eff}$. In addition, we compare the DMD performance of RCF to that of SIF. Through detailed numerical simulations based on the full-vector finite element method [15], we find that RCF realizes three-spatial-mode transmission which SIF cannot realize.

Manuscript received October 24, 2013; revised December 15, 2013; accepted February 3, 2014. Date of publication February 4, 2014; date of current version February 21, 2014.

M. Kasahara and K. Saitoh are with the Graduate School of Information Science and Technology, Hokkaido University, Sapporo 060–0814, Japan (e-mail: kasahara@icp.ist.hokudai.ac.jp; ksaitoh@ist.hokudai.ac.jp).

T. Sakamoto, N. Hanzawa, T. Matsui, K. Tsujikawa, and F. Yamamoto are with the Access Network Service Systems Laboratories, NTT Corporation, Tsukuba, Ibaraki 305–0805, Japan (e-mail: sakamoto.taiji@lab.ntt.co.jp; hanzawa.nobutomo@lab.ntt.co.jp; matsui.takashi@lab.ntt.co.jp; tujikawa.kyouzou@lab.ntt.co.jp; yamamoto.fumihiko@lab.ntt.co.jp).

Color versions of one or more of the figures in this paper are available online at http://ieeexplore.ieee.org.

Digital Object Identifier 10.1109/JLT.2014.2304732

II. Core Design

Schematic cross section and refractive index profile of RCF are shown in Fig. 1(a) and (b), respectively. The RCF's parameters are the core diameter $2a$, the diameter of the low refractive index region in the center of the core d, and the relative refractive index difference between the core and the cladding is defined as $\Delta = \left(n_{\rm core}^2 - n_{\rm clad}^2\right)/\left(2n_{\rm core}^2\right)$, where the background material

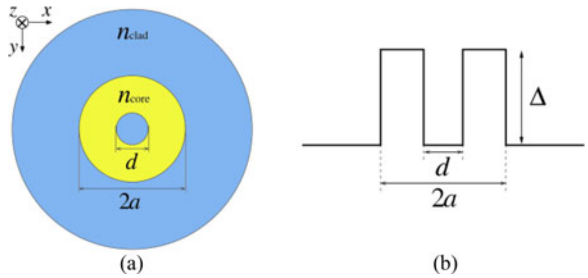

Fig. 1. (a) Schematic cross section and (b) refractive index profile.

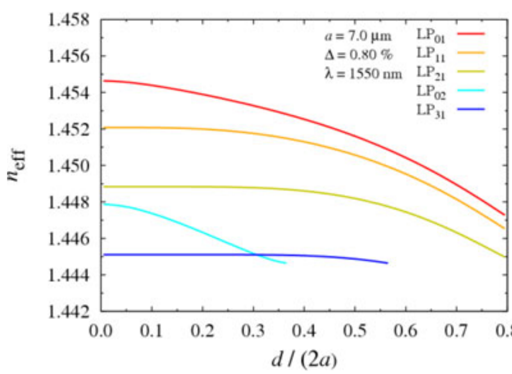

Fig. 2. Variation of the effective indices $(n_{\rm eff})$ of LP_{01}, LP_{11}, LP_{21}, LP_{02}, and LP_{31} modes in RCF with the core radius $a = 7.0$ μm and the relative refractive index difference $\Delta = 0.80\%$ as a function of the normalized diameter of the low refractive index region of $d/(2a)$ at the wavelength $\lambda = 1550$ nm.

is assumed to be silica and its refractive index is calculated with Sellmeier equation.

III. Characteristics of the Ring-Core Fiber

Fig. 2 shows variation of the effective indices $(n_{\rm eff})$ of LP_{01}, LP_{11}, LP_{21}, LP_{02}, and LP_{31} modes in RCF with the core radius $a = 7.0$ μm and the relative refractive index difference $\Delta = 0.80\%$ as a function of the normalized diameter of the low refractive index region of $d/(2a)$ at the wavelength $\lambda = 1550$ nm. Here, the structure of $d/(2a) = 0$ corresponds to SIF. We use full-vector finite element method [15] for modal analysis and don't employ linearly polarized approximation. However, we use "LP mode" as an only name of a propagation mode. As shown in Fig. 2, $n_{\rm eff}$ of all modes decrease as $d/(2a)$ becomes large. However, in the range that is smaller than $d/(2a) = 0.30$, only $n_{\rm eff}$ of LP_{01} and LP_{02} modes decrease. Therefore, $\Delta n_{\rm eff}$ between LP_{21} and LP_{02} modes is small in the structure of $d/(2a) = 0$, that is, SIF, but becomes large in the structure of $d/(2a) = 0.30$. From Fig. 3(a)–(e), we consider this characteristic. In the structure of $d/(2a) = 0.30$, mode field distribution of LP_{11}, LP_{21}, and LP_{31} modes are hardly affected by the low refractive index region as shown in Fig. 3(b), (c), and (e). Therefore, $n_{\rm eff}$ of LP_{11}, LP_{21}, and LP_{31} modes are approximately constant in the range that is smaller than $d/(2a) = 0.30$. In contrast, mode fields of LP_{01} and LP_{02} modes are distributed over the center of the core as shown in Fig. 3(a) and (d). Therefore, $n_{\rm eff}$ of LP_{01} and LP_{02} modes decrease as $d/(2a)$ becomes large. It should be noted that $n_{\rm eff}$ depends on both d and a, not just $d/(2a)$. However,

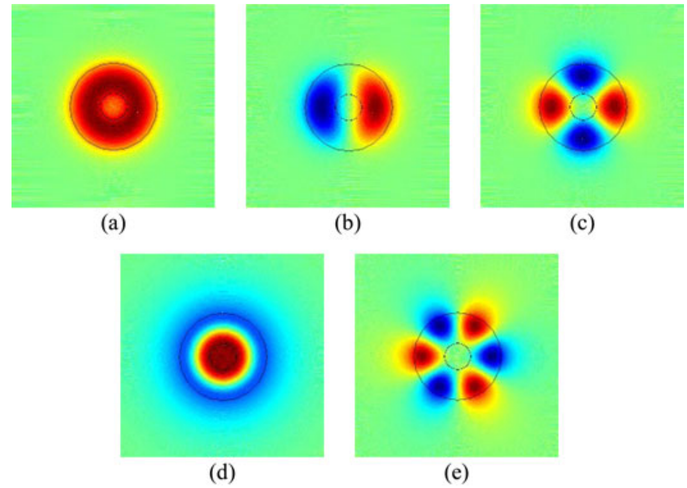

Fig. 3. Mode field distribution of (a) LP_{01}, (b) LP_{11}, (c) LP_{21}, (d) LP_{02}, and (e) LP_{31} modes in RCF with the core radius $a = 7.0$ μm, the relative refractive index difference $\Delta = 0.80\%$, and the normalized diameter of the low refractive index region of $d/(2a) = 0.30$.

it is necessary to control $d/(2a)$ because characteristics of RCFs almost depend on $d/(2a)$ as shown in subsequent sections. Fig. 4 shows normalized propagation constant b as a function of the normalized frequency V in (a) SIF and in RCF with (b) $d/(2a) = 0.20$, (c) 0.25, and (d) 0.30. Here, V and b are defined as

$$V = \frac{2\pi}{\lambda} a n_{\rm core} \sqrt{2\Delta} \tag{1}$$

$$b = \frac{n_{\rm eff}^2 - n_{\rm clad}^2}{n_{\rm core}^2 - n_{\rm clad}^2} \tag{2}$$

where λ is the wavelength. As shown in Fig. 4(a), we find that b of LP_{02} mode in SIF is close to that of LP_{21} mode even if V changes. In other words, $\Delta n_{\rm eff}$ between LP_{21} and LP_{02} modes remains small even if the fiber parameters change. In contrast, dispersion curve of LP_{02} mode in RCF shifts to the right with increasing the size of $d/(2a)$ as shown in Fig. 4(b)–(d). From the viewpoints of these characteristics, we expect that RCF realizes three-spatial-mode transmission by appropriately setting the fiber parameters.

IV. Design Condition

We investigate the region satisfying the design conditions for three-spatial-mode transmission over the C band from 1530 nm to 1565 nm. There are two requirements to ensure three-spatial-mode transmission. The first requirement is the elimination of the unexpected modes such as LP_{02} and LP_{31} modes. In order to guarantee the three-spatial-mode transmission, the BL of LP_{02} or LP_{31} mode, which is the high-order mode next to LP_{21} mode, is required to be larger than 1 dB/m at 1530 nm when the bending radius equals 140 mm. Here, the BL includes leakage losses. The second is the low BL of propagation modes such as LP_{01}, LP_{11}, and LP_{21} modes. In reference to ITU-T recommendations G.654, the BL of LP_{21} mode, which is one of the propagation modes, is required to be less than 0.5 dB/100 turns at 1565 nm when the bending radius equals 30 mm [16].

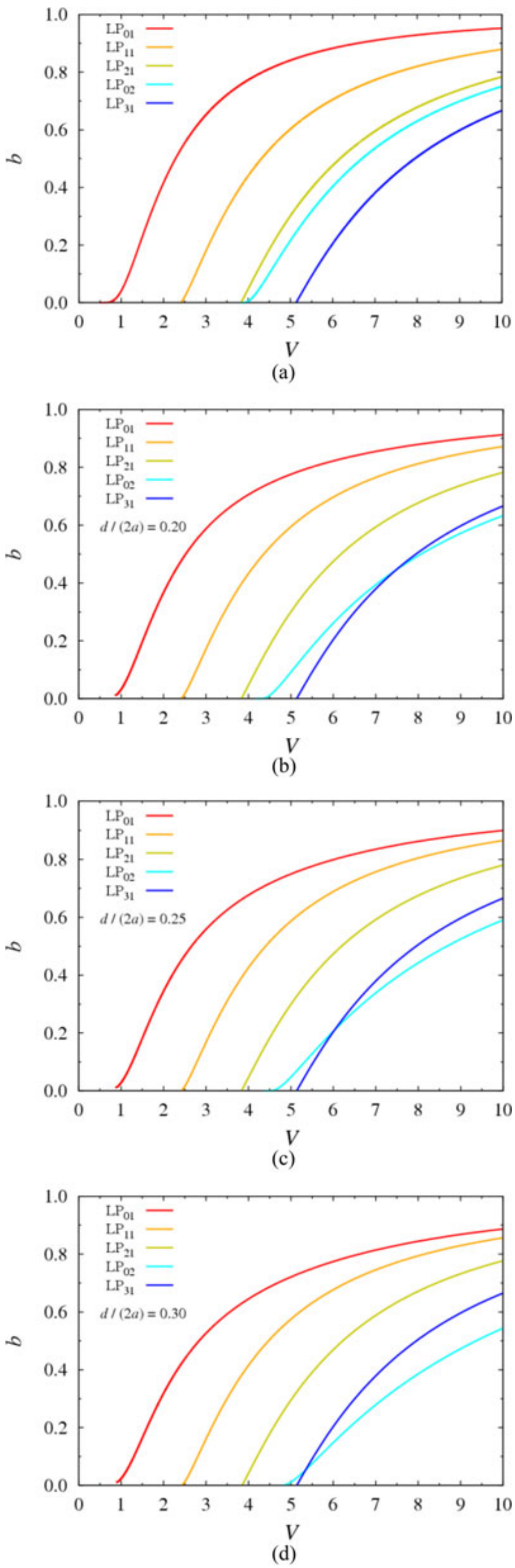

Fig. 4. Normalized propagation constant b as a function of the normalized frequency V in (a) SIF and in RCF with the normalized diameter of the low refractive index region of (b) $d/(2a) = 0.20$, (c) 0.25, and (d) 0.30.

In this paper, we refer to not ITU-T recommendations G.652 but G.654 because we assume the cut-off shifted fibers with 1550 nm central wavelength.

Fig. 5 shows structural parameter dependence of the design conditions in (a) SIF and in RCF with the normalized diameter of the low refractive index region of (b) $d/(2a) = 0.20$, (c) 0.25, and (d) 0.30. The light blue and blue curves indicate that the BL of LP_{02} and LP_{31} modes equal to 1 dB/m, respectively. The red curve indicates that the BL of LP_{21} mode equals to 0.5 dB/100 turns. To analyze the BL of fibers, we use full-vector finite element method [15]. In our modeling, a bent fiber is transformed into a straight fiber with equivalent refractive index method [17]. A perfectly matching layer is implemented at the fiber surface to emulate the effect of an infinite domain in the finite element model. With the perfectly matching layer, the propagation constant of a mode becomes complex. The BL is calculated as a product of the imaginary part of the propagation constant and one neper (Np). The cut-off of LP_{02} or LP_{31} condition is satisfied below the light blue or blue curve, respectively, whereas the low BL of LP_{21} condition is satisfied above the red curve. Therefore, the region painted with color satisfies the design conditions. As shown in Fig. 5(a), we find that SIF cannot meet the design conditions. We also find that the region satisfying the design conditions in RCFs might exist if the relative refractive index difference Δ is more than 1% with small core radius. However, Δ more than 1% is undesirable from the view point of optical fiber manufacturing. RCF can break this problem as shown in Fig. 5(b), (c) and (d). When we fix $d/(2a) = 0.25$ – 0.30, we find that the region satisfying the design conditions exists even if Δ is approximately 0.4%. Furthermore, the BL curves of LP_{31} and LP_{21} modes don't almost change as shown in Fig. 5(a)–(d). In contrast, the BL curve of LP_{02} mode shifts to the right with increasing the size of $d/(2a)$. On this account, the BL of LP_{02} mode becomes at the same level as that of LP_{31} mode when we fix $d/(2a) = 0.30$. In addition, if we fix the structure of $a = 7.0$ μm and $\Delta = 0.65\%$, we find that the region satisfying the design conditions exists in the range of $d/(2a) =$ 0.20 – 0.30.

V. Effective Area and Effective Index Difference

Fig. 6(a), (b), and (c) show structural parameter dependence of A_{eff} (LP_{01}) in RCF with the normalized diameter of the low refractive index region of (a) $d/(2a) = 0.20$, (b) 0.25, and (c) 0.30. The light blue, blue, and red curves correspond to those of Fig. 5. The black dashed lines correspond to Δn_{eff} between LP_{01} and LP_{11} modes. As shown in Fig. 6(a), (b), and (c), A_{eff} (LP_{01}) slightly enlarges as $d/(2a)$ becomes large. In contrast, Δn_{eff} between LP_{01} and LP_{11} modes decreases as $d/(2a)$ becomes large. Values of A_{eff} and Δn_{eff} are summarized in Table I. Here, these values are simulated in the structure of the core radius $a = 7.0$ μm and the relative refractive index difference $\Delta = 0.65\%$. Both A_{eff} (LP_{11}) and A_{eff} (LP_{21}) remain almost constant even if $d/(2a)$ changes as shown in Table I. In contrast, A_{eff} (LP_{01}) spreads under the influence of the low refractive index region in the center of the core as $d/(2a)$ becomes large. Fig. 6(d) shows normalized intensity of LP_{01} mode in SIF and

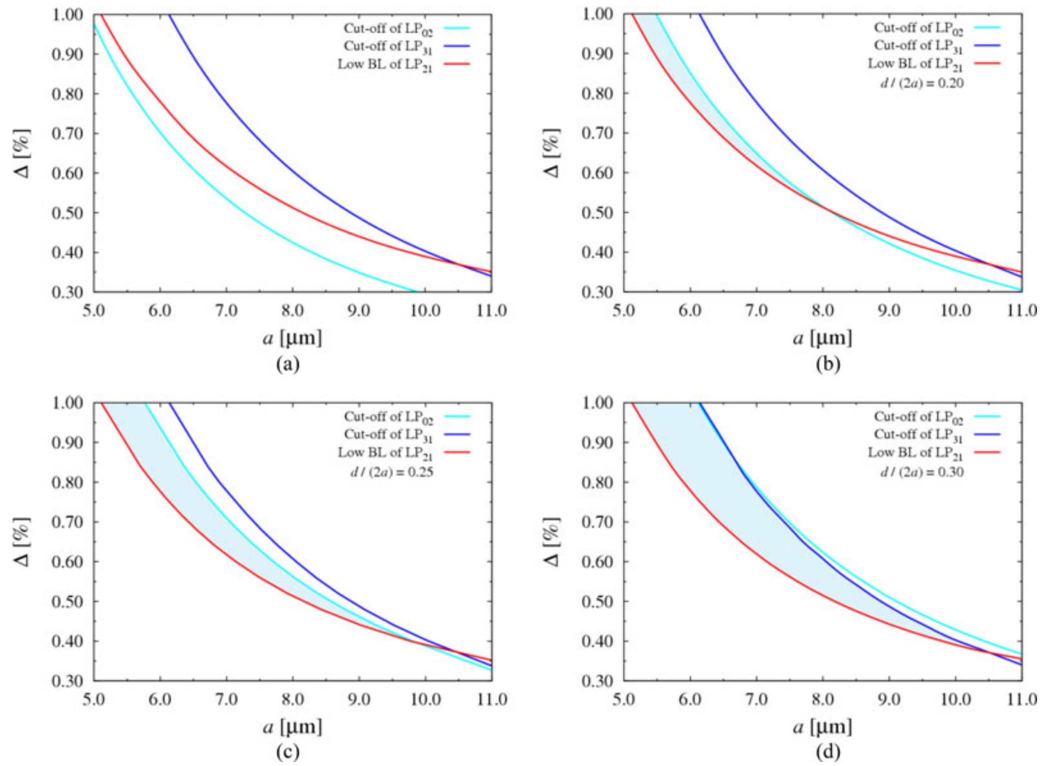

Fig. 5. Structural parameter dependence of the design conditions in (a) SIF and in RCF with the normalized diameter of the low refractive index region of (b) $d/(2a) = 0.20$, (c) 0.25, and (d) 0.30. The light blue and blue curves correspond to the upper limits of the BL of LP_{02} and LP_{31} modes, respectively. The red curve corresponds to the lower limits of the BL of LP_{21} mode.

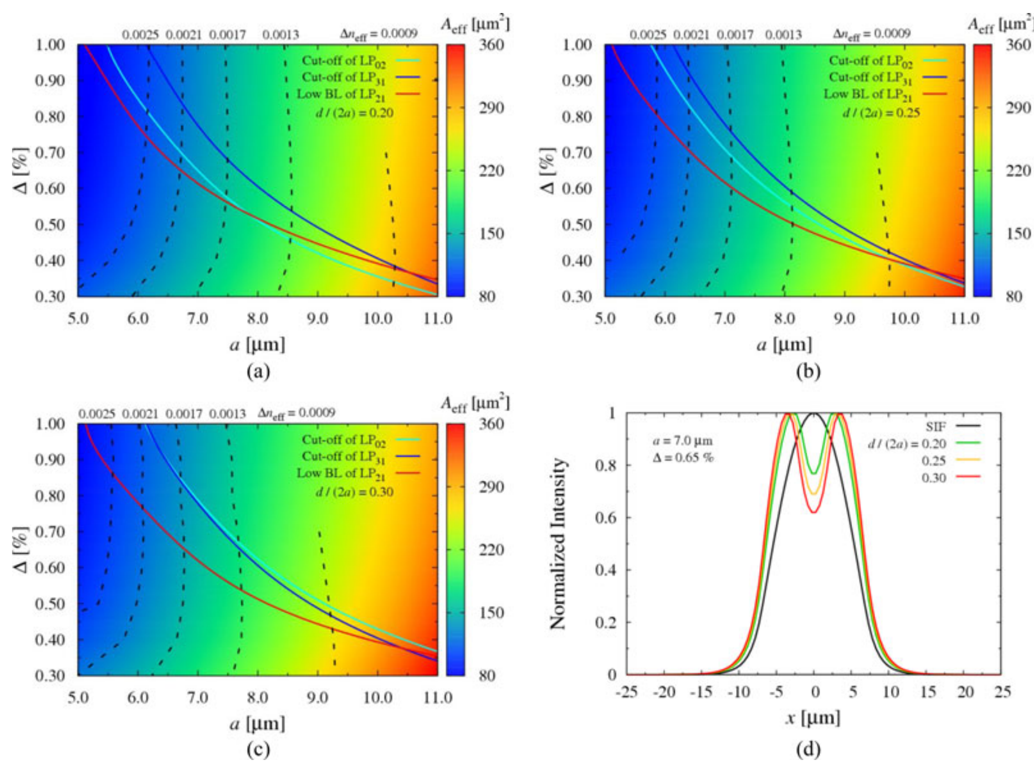

Fig. 6. Structural parameter dependence of $A_{\rm eff}$ (LP_{01}) in RCF with the normalized diameter of the low refractive index region of (a) $d/(2a) = 0.20$, (b) 0.25, and (c) 0.30. The light blue, blue, and red curves correspond to those of Fig. 5. The black dashed lines correspond to $\Delta n_{\rm eff}$ between LP_{01} and LP_{11} modes. (d) Normalized intensity of LP_{01} mode in SIF and in RCF with $d/(2a) = 0.20$, 0.25, and 0.30.

TABLE I
VALUES OF EFFECTIVE AREA AND EFFECTIVE INDEX DIFFERENCE

$d/(2a)$	0.20	0.25	0.30
A_{eff} (LP_{01}) [μm^2]	137	144	150
A_{eff} (LP_{11}) [μm^2]	164	164	165
A_{eff} (LP_{21}) [μm^2]	193	193	193
Δn_{eff} (LP_{01} – LP_{11})	1.94×10^{-3}	1.75×10^{-3}	1.59×10^{-3}
Δn_{eff} (LP_{11} – LP_{21})	3.04×10^{-3}	2.97×10^{-3}	2.89×10^{-3}

in RCF with $d/(2a) = 0.20$, 0.25, and 0.30. Here, x indicates the position from the center of the core. The normalized intensity of LP_{01} mode in SIF is Gaussian distribution, whereas that in RCF has a dip in the center of the core as shown in Fig. 6(d). Additionally, the dip becomes deeper as $d/(2a)$ becomes large.

Besides A_{eff}, other characteristic to be considered for few-mode fibers is mode coupling between propagation modes. Mode coupling depends on a lot of factors, including mode profiles and fiber fabrication. It is known that the large Δn_{eff} minimizes the mode coupling. With respect to the relationship between Δn_{eff} and the mode coupling, Refs. [18] and [6] indicate that mode coupling of the fibers with Δn_{eff} of 1.3×10^{-3} and 2.8×10^{-3} are 18.2 dB for 500 m (3.64×10^{-2} dB/m) and 25 dB for 30 km (8.33×10^{-4} dB/m), respectively. As shown in Fig. 6(a), (b), and (c), Δn_{eff} larger than 2.5×10^{-3} can be realized on condition that Δ is less than 1%. Additionally, Δn_{eff} between LP_{11} and LP_{21} modes is larger than that of between LP_{01} and LP_{11} modes as shown in Table I. Besides, if we fix core parameters, Δn_{eff} between propagation modes in RCF is smaller than that in SIF as shown in Fig. 2. Also, Δn_{eff} between propagation modes becomes large with decreasing core diameter as shown in Fig. 6(a)–(c). This means that the core diameter of RCF is always smaller than that of SIF for given Δn_{eff}. Therefore, we expect that the mode coupling is small in the region that a is small and Δ is large. However, we also find that there is a trade-off between A_{eff} and Δn_{eff}. On this account, we should choose the optimum structure to satisfy the desired values of A_{eff} and Δn_{eff}.

VI. DIFFERENTIAL MODE DELAY

DMD is important for reduction of complexity and power consumption of MIMO processing. We defined the DMD between LP_{01} and LP_{11} modes as a value that subtracted the group delay τ of the LP_{01} mode from that of the LP_{11} mode, which is expressed as follows:

$$\mathrm{DMD} = \tau_{\mathrm{LP11}} - \tau_{\mathrm{LP01}} = \frac{n_{\mathrm{g11}} - n_{\mathrm{g01}}}{c} = \frac{n_{\mathrm{eff11}} - n_{\mathrm{eff01}}}{c} - \frac{\lambda}{c}\left(\frac{\partial n_{\mathrm{eff11}}}{\partial \lambda} - \frac{\partial n_{\mathrm{eff01}}}{\partial \lambda}\right) \quad (3)$$

where n_{g01} and n_{g11} are the group indices of LP_{01} and LP_{11} modes, c is the light velocity in a vacuum and λ means the free space wavelength. Fig. 7 shows variation of DMD with the core radius $a = 7.0$ μm and the relative refractive index difference $\Delta = 0.65\%$ as a function of the normalized diameter of the low refractive index region of $d/(2a)$. The solid and dashed curves correspond to DMD between LP_{01} and LP_{11} modes, between LP_{01} and LP_{21} modes, respectively. The blue and red curves correspond to DMD at the wavelength $\lambda = 1530$ nm and 1565 nm, respectively. Here, the structure of $d/(2a) = 0$ corresponds to SIF. As shown in Fig. 7, we find that the DMD in RCF is larger than in SIF. This is because τ_{LP01} becomes small by an influence of the low refractive index region in the center of the core. We also find that the DMD decreases in the range that $d/(2a)$ is relatively large. This is because not only τ_{LP01} but also τ_{LP11} and τ_{LP21} are affected by the low refractive index region in the center of the core. It is well-known that graded-index profile realizes reduction of DMD. In contrast, DMD in RCF is quit larger than that in graded-index fiber, which may result in requiring higher complexity at MIMO equalizers when we compensate for the mode crosstalk occurred at a mode multi/demultiplexer or splice points. However, Ref. [19] proposes a mode-division multiplexing system with reduced MIMO processing complexity, whose computational complexity is independent of the DMD value of the fiber. Therefore, we believe that MIMO processing complexity can be kept low even with the high DMD fiber such as RCF, when adopting the equalizer described in [19].

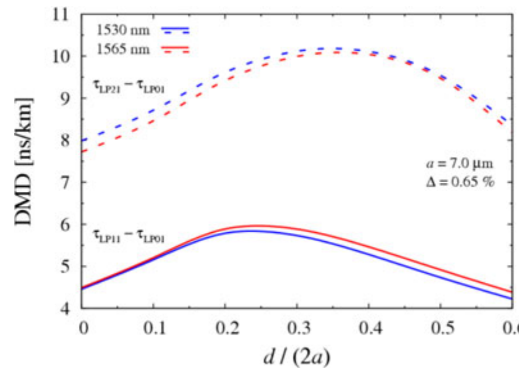

Fig. 7. Variation of DMD with the core radius $a = 7.0$ μm and the relative refractive index difference $\Delta = 0.65\%$ as a function of the normalized diameter of the low refractive index region of $d/(2a)$. The solid and dashed curves correspond to DMD between LP_{01} and LP_{11} modes, between LP_{01} and LP_{21} modes, respectively. The blue and red curves correspond to the DMD at the wavelength $\lambda = 1530$ nm and 1565 nm, respectively.

VII. CONCLUSION

The region satisfying the design conditions for three-spatial-mode transmission has been investigated in RCF. We have also evaluated the relationship between A_{eff} and Δn_{eff} in RCF. In addition, we have evaluated DMD of RCF compared to SIF. Through detailed numerical simulations, we found that RCF suppresses the LP_{02} mode selectively under the influence of the low refractive index region in the center of the core. On this account, we also found that RCF realizes three-spatial-mode transmission which SIF cannot realize. With respect to A_{eff} (LP_{01}), we could choose a desired value from about 80 μm^2 to about 360 μm^2 by adjusting the fiber parameters. With respect to Δn_{eff}, by selecting the structure of small A_{eff}, Δn_{eff} larger than 2.5×10^{-3} could be realized on condition that Δ is less than 1%. Finally, the influence of mode field distortion of LP_{01} mode is a subject for future analysis.

REFERENCES

[1] N. Hanzawa, K. Saitoh, T. Sakamoto, T. Matsui, S. Tomita, and M. Koshiba, “Demonstration of mode-division multiplexing transmission over 10 km two-mode fiber with mode coupler,” in *Proc. Opt. Fiber Commun. Conf. Expo. Nat. Fiber Opt. Eng. Conf.*, 2011, Paper OWA4.

[2] E. Ip, M. J. Li, K. Bennett, Y. K. Huang, A. Tanaka, A. Korolev, K. Koreshkov, W. Wood, E. Mateo, J. Hu, and Y. Yano, “146λx6 × 19-Gbaud wavelength-and-mode-division multiplexed transmission over 10 × 50-km spans of few-mode fiber with a gain-equalized few-mode EDFA,” in *Proc. Opt. Fiber Commun. Conf. Expo. Nat. Fiber Opt. Eng. Conf.*, 2013, Paper PDP5 A.2.

[3] M. Salsi, C. Koebele, G. Charlet, and S. Bigo, “Mode division multiplexed transmission with a weakly-coupled few-mode fiber,” in *Proc. Opt. Fiber Commun. Conf. Expo. Nat. Fiber Opt. Eng. Conf.*, 2012, Paper OTU2 C.5.

[4] R. Ryf, S. Randel, N. K. Fontaine, M. Montoliu, E. Burrows, S. Corteslli, S. Chandrasekhar, A. H. Gnauck, C. Xie, R.-J. Essiambre, P. J. Winzer, R. Delbue, P. Pupalaikis, A. Sureka, Y. Sun, L. Gruner-Nielsen, R. V. Jensen, and R. Lingle, “32-bit/s/Hz spectral efficiency WDM transmission over 177-km few-mode-fiber,” in *Proc. Opt. Fiber Commun. Conf. Expo. Nat. Fiber Opt. Eng. Conf.*, 2013, Paper PDP5 A.1.

[5] F. Ferreira, D. Fonseca, and H. Silva, “Design of few-mode fibers with arbitrary and flattened differential mode delay,” *IEEE Photon. Technol. Lett.*, vol. 25, no. 5, pp. 438–441, Mar. 2013.

[6] L. Gruner-Nielsen, Y. Sun, J. Nicholson, D. Jakobsen, K. Jespersen, R. Lingle, and B. Palsdottir, “Few mode transmission fiber with low DGD, low mode coupling, and low loss,” *J. Lightw. Technol.*, vol. 30, no. 23, pp. 3693–3698, Dec. 2012.

[7] R. Olshansky, “Mode coupling effects in graded-index optical fiber,” *Appl. Opt.*, vol. 14, no. 4, pp. 935–945, Apr. 1975.

[8] P. Sillard, M. Bigot-Astruc, D. Boivin, H. Maerten, and L. Provost, “Few-mode fiber for uncoupled mode-division multiplexing transmissions,” in *Proc. Eur. Conf. Opt. Commun.*, 2011, Paper Tu.5.LeCervin.7.

[9] K. Mukasa, K. Imamura, R. Sugizaki, and T. Yagi, “Comparisons of merits on wide-band transmission systems between using extremely improved solid SMFs with $A_{\rm eff}$ of 160 μm^2 and loss of 0.175 dB/km and using large-$A_{\rm eff}$ holey fibers enabling transmission over 600 nm bandwidth,” in *Proc. Opt. Fiber Commun. Conf. Expo. Nat. Fiber Opt. Eng. Conf.*, 2008, Paper OThR1.

[10] T. Matsui, T. Sakamoto, K. Tsujikawa, S. Tomita, and M. Tsubokawa, “Single-mode photonic crystal fiber design with ultralarge effective area and low bending loss for ultrahigh-speed WDM transmission,” *J. Lightw. Technol.*, vol. 29, no. 4, pp. 511–515, Feb. 2011.

[11] M. Bigot-Astruc, L. Provost, G. Krabshuis, P. Dhenry, and P. Sillard, “125 μm glass diameter single-mode fiber with Aeff of 155 μm^2,” in *Proc. Opt. Fiber Commun. Conf. Expo. Nat. Fiber Opt. Eng. Conf.*, 2011, Paper OTuJ2.

[12] N. K. Fontaine, R. Ryf, M. Hirano, and T. Sasaki, “Experimental investigation of crosstalk accumulation in a ring-core fiber,” in *Proc. IEEE Summer Topicals*, 2013, Paper TuC4.2.

[13] X. Q. Jin, R. Li, D. C. O’Brien, and F. P. Payne, “Linearly polarized mode division multiplexed transmission over ring-index multimode fibres,” in *Proc. IEEE Summer Topicals*, 2013, Paper TuC4.3.

[14] J. Marcou and S. Février, “On the analysis of a weakly guiding doubly clad dielectric optical fiber with an annular core,” *Microw. Opt. Technol. Lett.*, vol. 38, pp. 249–254, Aug. 2003.

[15] K. Saitoh and M. Koshiba, “Full-vectorial imaginary-distance beam propagation method based on a finite element scheme: application to photonic crystal fibers,” *IEEE J. Quantum Electron.*, vol. 38, no. 7, pp. 927–933, Jul. 2002.

[16] *Characteristics of a Cut-Off Shifted, Single-Mode Fibre and Cable*, ITU-T Standard G.654, Oct. 2012.

[17] M. Heiblum and J. H. Harris, “Analysis of curved optical waveguides by conformal transformation,” *IEEE J. Quantum Electron.*, vol. 11, no. 2, pp. 75–83, Feb. 1975.

[18] K. Jespersen, Z. Li, L. Gruner-Nielsen, B. Palsdottir, F. Poletti, and J. W. Nicholson, “Measuring distributed mode scattering in long few-moded fibers,” in *Proc. Opt. Fiber Commun. Conf. Expo. Nat. Fiber Opt. Eng. Conf.*, 2012, Paper OTh3 I.4.

[19] T. Sakamoto, T. Mori, T. Yamamoto, N. Hanzawa, S. Tomita, F. Yamamoto, K. Saitoh, and M. Koshiba, “Mode-division multiplexing transmission system with DMD-independent low complexity MIMO processing,” *J. Lightw. Technol.*, vol. 31, no. 13, pp. 2192–2199, Jul. 2013.

Motoki Kasahara was born in Hokkaido, Japan, on June 24, 1989. He received the B.S. degree in electronic engineering from Hokkaido University, Sapporo, Japan, in 2012, where he is currently working toward the M.S. degree in media and network technologies.

His research interests include the modeling of few-mode fiber using the finite-element method. Mr. kasahara is a member of the Institute of Electronics, Information and Communication Engineers of Japan.

Kunimasa Saitoh (S’00–M’01) received the B.S., M.S., and Ph.D. degrees in electronic engineering from Hokkaido University, Sapporo, Japan, in 1997, 1999, and 2001, respectively.

From 1999 to 2001, he was a Research Fellow of the Japan Society for the Promotion of Science. From 2001 to 2005, he was a Research Associate at the Graduate School of Engineering, Hokkaido University. From 2005 to 2013, he was an Associate Professor at the Graduate School of Information Science and Technology, Hokkaido University, and in 2013, he became a Professor there. He has been engaged in research on fiber optics, nanophotonics, integrated optical devices, and computer-aided design and modeling of guided-wave devices using finite element method, beam propagation method, and so on. He is an author or coauthor of more than 150 research papers in refereed international journals.

Dr. Saitoh is a member of the Optical Society of America, and the Institute of Electronics, Information and Communication Engineers. In 1999 and 2002, he received the Excellent Paper Award and the Young Scientist Award from the IEICE, respectively, and in 2008, the Young Scientists’ Prize of the Commendation for Science and Technology from the Ministry of Education, Culture, Sports, Science, and Technology, Government of Japan. From 2009 to 2010, he served as a Secretary/Treasurer of the IEEE Sapporo Section.

Taiji Sakamoto received the B.E., M.E., and Ph.D. degrees in electrical engineering from Osaka Prefecture University, Osaka, Japan, in 2004, 2006, and 2012, respectively.

In 2006, he joined NTT Access Network Service Systems Laboratories, NTT, Ibaraki, Japan, where he has been engaged in research on optical fiber design and optical nonlinear effects in optical fiber.

Dr. Sakamoto is a member of the Institute of Electronics, Information and Communication Engineers.

Nobutomo Hanzawa received the B.E. and M.E. degrees in electrical engineering from Yamagata University, Yonezawa, Japan, in 2005 and 2007, respectively.

Since 2007, he has been in the NTT Access Network Service Systems Laboratories, NTT Corporation, Tsukuba, Japan. He has been engaged in research on optical fiber design.

Mr. Hanzawa is a member of the Institute of Electronics, Information, and Communication Engineers of Japan.

Takashi Matsui received B.E., M.E., and Ph. D. degrees in electronic engineering from Hokkaido University, Sapporo, Japan, in 2001, 2003 and 2008, respectively. He also attained the status of Professional Engineer (P.E.Jp) in electrical and electronic engineering in 2009. In 2003, he joined NTT Access Network Service Systems Laboratories, Ibaraki, Japan. He has been engaged in research on optical fiber design techniques.

Dr. Matsui is a member of the Institute of Electronics, Information and Communication Engineers of Japan.

Kyozo Tsujikawa received the B.S. and M.S. degrees in chemistry, and the Dr. Eng. degree from the Tokyo Institute of Technology in 1990, 1992, and 2006, respectively.

Since joining NTT, he has undertaken research on glasses for low-loss optical fibers and worked on the measurement of the optical fibers and worked on the measurement of the optical properties of fiber cables. He is now a Senior Research Engineer, NTT Access Network Service Systems Laboratories, Tsukuba, Ibaraki, Japan.

Dr. Tsujikawa is a member of the Institute of Electronics, Information and Communication Engineers of Japan.

Fumihiko Yamamoto received the B.E., M.E., and Dr. Eng. degrees from Kyusyu University, Fukuoka, Japan, in 1989, 1991 and 2001, respectively. In 1991, he joined NTT Transmission Systems Laboratories, Ibaraki, Japan. During his 21-year career at NTT, he has been engaged in research and development on optical access network design, and has planned and driven the strategy for introducing NTT's research and development technologies. Since 2012, he has been managing the Optical Fiber Research Group, NTT Access Network Systems Laboratories as a Senior Research engineer.

Mr. Yamamoto is a member of the Institute of Electronics, Information and Communication Engineers of Japan.